Electronic Supplementary Information for:

Effects of linking units on fused-ring electron acceptor dimers

Guilong Cai,[a,b] Yiqun Xiao,[c] Mengyang Li,[d] Jeromy James Rech,[e] Jiayu Wang,[b] Kuan Liu,[b] Xinhui Lu,[c] Zheng Tang,[d] Jiarong Lian,*[a] Pengju Zeng,[a] Yiping Wang,[a] Wei You[e] and Xiaowei Zhan*[b]

[a] Key Laboratory of Optoelectronic Devices and Systems of Ministry of Education and Guangdong Province, College of Physics and Optoelectronic Engineering, Shenzhen University, Shenzhen 518060, China. E-mail: ljr@szu.edu.cn

[b] Department of Materials Science and Engineering, College of Engineering, Key Laboratory of Polymer Chemistry and Physics of Ministry of Education, Peking University, Beijing 100871, China. E-mail: xwzhan@pku.edu.cn

[c] Department of Physics, The Chinese University of Hong Kong, New Territories 999077, Hong Kong, China.

[d] Center for Advanced Low-dimension Materials, State Key Laboratory for Modification of Chemical Fibers and Polymer Materials, College of Materials Science and Engineering, Donghua University, Shanghai 201620, China.

[e] Department of Chemistry, University of North Carolina at Chapel Hill, Chapel Hill, North Carolina 27599, United States.

Materials

Unless stated otherwise, all the chemical reagents and solvents used were obtained commercially and were used without further purification. Chloroform (99.9%), 1, 8-diiodooctane (DIO) (97.0%) and 2-methoxyethanol (99.8%) were purchased from TCI and J&K Chemical Inc.; $Zn(CH_3COO)_2 \cdot 2H_2O$ (99.0%), ethanolamine (99.5%) and MoO_3 were purchased from Sigma-Aldrich Inc. Toluene and tetrahydrofuran (THF) were distilled from sodium benzophenone under nitrogen. Compounds **1**, **4**, **5** and **6** were purchased from Sunatech Ltd and TCI. 2FIC[S1] and FTAZ[S2] were synthesized according to our published procedures.

Synthesis

Compound 2. To a stirred solution of compound **1** (500 mg, 0.83 mmol, 1.0 eq.) in 1,2-dichloroethane (DCE, 20 mL) at 0 °C, *N,N*-dimethylformamide (DMF) (0.2 mL, 2.5 mmol, 3.0 eq.) and phosphorous oxychloride ($POCl_3$) (0.12 mL, 1.2 mmol, 1.5 eq.) was added dropwise sequentially under argon protection. Then, the mixture was stirred at room temperature for 12 h. The reaction was quenched by sodium acetate solution. The organic layer was separated and the aqueous layer was extracted with dichloromethane (2 × 50 mL). The combined organic phases were washed with brine, dried over $MgSO_4$, and concentrated. The crude product was purified by silica gel column chromatography (petroleum ether/dichloromethane, v/v = 3/1) to give a yellow solid (433 mg, 83%). ^{1}H NMR (300 MHz, $CDCl_3$): δ 9.89 (s, 1H), 7.62 (s, 1H), 7.41 (s, 1H), 7.37 – 7.29 (m, 2H), 6.98 (d, J = 4.8 Hz, 1H), 2.06 – 1.83 (m, 8H), 1.15 – 1.09 (m, 24H), 0.83 – 0.75 (m, 20H). ^{13}C NMR (75 MHz, $CDCl_3$): δ 183.0,

156.6, 155.1, 155.0, 154.0, 152.8, 144.5, 141.2, 138.7, 133.9, 130.7, 127.9, 121.9, 115.0, 113.3, 54.2, 54.0, 39.2, 31.7, 29.7, 24.3, 24.2, 22.7, 14.1. MS (MALDI-TOF): *m/z* 631.4 (M^+). Anal. calcd for $C_{41}H_{58}OS_2$: C, 78.04; H, 9.26. Found: C, 78.13; H, 9.34.

Compound 3. To a stirred solution of compound **2** (150 mg, 0.24 mmol, 1.0 eq.) in dry DMF (5 mL) was added NBS (80 mg, 0.43 mmol, 1.8 eq.) under argon and the mixture was stirred at room temperature for 2 h. After aqueous $Na_2S_2O_3$ was added, the organic layer was separated. The aqueous layer was extracted with dichloromethane (2 × 50 mL). The combined organic phases were washed with brine, dried over $MgSO_4$ and concentrated. The crude product was purified by silica gel column chromatography (petroleum ether/dichloromethane, v/v = 2/1) to give bright yellow solid (116 mg, 68%). ^{1}H NMR (300 MHz, $CDCl_3$): δ 9.89 (s, 1H), 7.62 (s, 1H), 7.39 (s, 1H), 7.24 (s, 1H), 7.00 (s, 1H), 2.06 – 1.81 (m, 8H), 1.17 – 1.06 (m, 24H), 0.86 – 0.75 (m, 20H). ^{13}C NMR (75 MHz, $CDCl_3$): δ 183.0, 155.4, 155.3, 155.1, 152.7, 152.5, 144.8, 141.6, 138.1, 134.2, 130.6, 125.0, 115.0, 114.1, 113.2, 55.0, 54.2, 39.1, 39.1, 31.7, 31.7, 29.7, 24.3, 24.2, 22.7, 22.7, 14.1. MS (MALDI-TOF): *m/z* 709.3 (M^+). Anal. calcd for $C_{41}H_{57}BrOS_2$: C, 69.37; H, 8.09. Found: C, 69.27; H, 7.91.

SID-CHO. To a three-necked round bottom flask were added compound **3** (142 mg, 0.2 mmol, 2.0 eq.), compound **4** (58 mg, 0.1 mmol, 1.0 eq.) and toluene (20 mL). The mixture was deoxygenated with nitrogen for 30 min. $Pd(PPh_3)_4$ (12 mg, 0.01 mmol, 0.1 eq.) was added under nitrogen. The mixture was refluxed for 48 h and then

cooled down to room temperature. Water (25 mL) was added and the mixture was extracted with chloroform (2 × 50 mL). The organic phase was dried over anhydrous $MgSO_4$ and filtered. After removal of the solvent under reduced pressure, the residue was purified by column chromatography on silica gel (petroleum ether/dichloromethane, v/v = 1/2) to give an orange red solid (100 mg, 82%). ^{1}H NMR (400 MHz, CD_2Cl_2): δ 9.88 (s, 2H), 7.66 (s, 2H), 7.49 (s, 2H), 7.37 (s, 2H), 7.20 (s, 2H), 2.11 – 1.91 (m, 16H), 1.27 (s, 16H), 1.18 – 1.08 (m, 48H), 0.80 – 0.75 (m, 24H). ^{13}C NMR (100 MHz, CD_2Cl_2): δ 183.3, 157.9, 155.9, 155.7, 154.0, 152.7, 145.3, 141.6, 140.6, 138.8, 134.7, 131.2, 118.4, 115.4, 113.7, 55.0, 54.8, 39.7, 39.6, 32.2, 32.2, 30.2, 30.2, 24.8, 24.7, 23.2, 23.1, 14.4. MS (MALDI-TOF): *m/z* 1258.7 (M^+). Anal. calcd for $C_{82}H_{114}O_2S_4$: C, 78.16; H, 9.12. Found: C, 78.18; H, 9.17.

DID-CHO. To a three-necked round bottom flask were added compound **3** (142 mg, 0.2 mmol, 2.0 eq.), compound **5** (61 mg, 0.1 mmol, 1.0 eq.) and toluene (20 mL). The mixture was deoxygenated with nitrogen for 30 min. $Pd(PPh_3)_4$ (12 mg, 0.01 mmol, 0.1 equiv.) was added under nitrogen. The mixture was refluxed for 48 h and then cooled down to room temperature. Water (25 mL) was added and the mixture was extracted with chloroform (2 × 50 mL). The organic phase was dried over anhydrous $MgSO_4$ and filtered. After removal of the solvent under reduced pressure, the residue was purified by column chromatography on silica gel (petroleum ether/dichloromethane, v/v = 1/2) to give a red solid (98 mg, 76%). ^{1}H NMR (400 MHz, CD_2Cl_2): δ 9.88 (s, 2H), 7.65 (s, 2H), 7.47 (s, 2H), 7.36 (s, 2H), 7.16 (s, 2H), 7.01 (s, 2H), 2.12 – 1.85 (m, 16H), 1.22 – 1.05 (m, 48H), 0.91 – 0.72 (m, 40H). ^{13}C

NMR (100 MHz, CD_2Cl_2): δ 183.3, 157.7, 155.9, 155.7, 154.3, 152.7, 146.5, 145.3, 141.0, 138.9, 134.8, 131.2, 122.0, 121.5, 115.4, 113.8, 54.8, 54.8, 39.7, 32.2, 32.2, 30.2, 30.2, 24.8, 24.8, 23.2, 23.1, 14.4, 14.4. MS (MALDI-TOF): *m/z* 1285.9 (M^+). Anal. calcd for $C_{84}H_{116}O_2S_4$: C, 78.45; H, 9.09. Found: C, 79.02; H, 9.14.

TID-CHO. Compound **3** (175 mg, 0.25 mmol, 2.3 eq.), compound **6** (30 mg, 0.11 mmol, 1.0 eq.), $Pd(OAc)_2$ (3.6 mg, 0.016 mmol, 0.14 eq.), Xphos (15.0 mg, 0.032 mmol, 0.28 eq.), K_3PO_4 (139.9 mg, 0.66 mmol, 6.0 eq.) were dissolved in deoxygenated THF (20 mL). The solution mixture was stirred at 80 °C for 48 h, and then cooled to room temperature. 25 mL of water was added and the mixture was extracted with dichloromethane (2 × 50 mL). The organic phase was dried over anhydrous $MgSO_4$ and filtered. After removal of the solvent under reduced pressure, the residue was purified by column chromatography on silica gel (petroleum ether/dichloromethane, v/v = 1/2) to give an orange solid (93 mg, 66%). ^{1}H NMR (400 MHz, CD_2Cl_2): δ 9.89 (s, 2H), 7.66 (s, 2H), 7.50 (s, 2H), 7.41 (s, 2H), 7.23 (s, 2H), 2.08 – 1.92 (m, 16H), 1.19 – 1.08 (m, 48H), 0.88 – 0.75 (m, 40H). ^{13}C NMR (100 MHz, CD_2Cl_2): δ 183.3, 156.6, 156.1, 155.7, 154.8, 152.4, 145.6, 144.2, 138.3, 135.4, 131.2, 127.4, 125.3, 115.5, 114.2, 89.5, 55.0, 54.8, 39.7, 32.2, 32.2, 30.2, 24.8, 23.2, 23.1, 14.4. MS (MALDI-TOF): *m/z* 1282.9 (M^+). Anal. calcd for $C_{84}H_{114}O_2S_4$: C, 78.57; H, 8.95. Found: C, 78.46; H, 8.88.

SIDIC. To a three-necked round bottom flask were added SID-CHO (100 mg, 0.08 mmol, 1.0 eq.), 2FIC (69 mg, 0.3 mmol, 3.8 eq.), pyridine (0.15 mL) and chloroform (20 mL). The mixture was deoxygenated with nitrogen for 20 min and

then stirred at reflux for 12 h. After cooling to room temperature, the mixture was poured into methanol (200 mL) and filtered. The residue was purified by column chromatography on silica gel (petroleum ether/dichloromethane, v/v = 1/1) to give a blue solid (118 mg, 85%). ^{1}H NMR (500 MHz, $CDCl_3$): δ 8.96 (s, 2H), 8.61 – 8.49 (m, 2H), 7.68 (dd, J = 16.3, 8.9 Hz, 4H), 7.56 (s, 2H), 7.31 (s, 2H), 7.19 (s, 2H), 2.18 – 1.82 (m, 16H), 1.39 – 0.82 (m, 64H), 0.82 – 0.72 (m, 24H). ^{13}C NMR (125 MHz, $CDCl_3$): δ 186.2, 159.0, 157.3, 156.9, 154.3, 153.4, 142.5, 140.0, 138.8, 136.7, 134.7, 119.8, 118.2, 116.1, 115.1, 114.9, 113.4, 112.6, 112.5, 68.2, 54.5, 54.4, 39.3, 39.1, 31.7, 29.8, 29.7, 24.5, 24.4, 22.7, 22.7, 14.1. HRMS calcd for $C_{106}H_{118}F_4N_4O_2S_4$: 1683.8107; found: 1683.8091. Anal. calcd for $C_{106}H_{118}F_4N_4O_2S_4$: C, 75.59; H, 7.06; N, 3.33. Found: C, 75.81; H, 6.96; N, 3.27.

DIDIC. Compound DIDIC was synthesized according to the synthetic procedure of compound SIDIC. Compound DIDIC was obtained as a blue solid (138 mg, 81%). ^{1}H NMR (500 MHz, $CDCl_3$): δ 8.95 (s, 2H), 8.54 (dd, J = 10.0, 6.4 Hz, 2H), 7.68 (dd, J = 15.4, 7.8 Hz, 4H), 7.54 (s, 2H), 7.30 (s, 2H), 7.17 (s, 2H), 7.01 (s, 2H), 2.13 – 1.88 (m, 16H), 1.26 – 1.02 (m, 48H), 0.96 – 0.71 (m, 40H). ^{13}C NMR (125 MHz, $CDCl_3$): δ 186.0, 164.3, 158.8, 158.6, 157.1, 156.7, 155.4, 155.3, 154.4, 153.3, 153.2, 147.3, 140.7, 140.5, 139.9, 138.6, 136.5, 136.5, 134.5, 134.0, 129.9, 122.0, 121.0, 119.6, 115.9, 115.0, 114.8, 114.7, 113.3, 112.5, 112.3, 67.9, 65.6, 54.2, 54.1, 39.2, 39.0, 31.6, 31.5, 29.6, 29.6, 24.3, 24.2, 22.5, 14.0, 14.0. HRMS calcd for $C_{108}H_{120}F_4N_4O_2S_4$: 1709.8263; found: 1709.8252. Anal. calcd for $C_{108}H_{120}F_4N_4O_2S_4$: C, 75.84; H, 7.07; N, 3.28. Found: C, 75.61; H, 7.16; N, 3.11.

TIDIC. Compound TIDIC was synthesized according to the synthetic procedure of compound SIDIC. Compound TIDIC was obtained as a blue solid (104 mg, 87%). ^{1}H NMR (500 MHz, $CDCl_3$): δ 8.96 (s, 2H), 8.55 (dd, J = 10.0, 6.2 Hz, 2H), 7.69 (dd, J = 16.0, 8.6 Hz, 4H), 7.56 (s, 2H), 7.35 (s, 2H), 7.24 (s, 2H), 2.12 – 1.88 (m, 16H), 1.27 – 1.02 (m, 48H), 0.96 – 0.72 (m, 40H). ^{13}C NMR (125 MHz, $CDCl_3$): δ 186.2, 163.8, 158.9, 157.4, 157.1, 156.9, 155.0, 143.6, 140.2, 138.9, 138.8, 136.7, 134.7, 127.0, 126.2, 120.1, 116.2, 115.2, 115.0, 114.8, 113.9, 112.7, 89.9, 68.5, 54.5, 54.5, 39.3, 39.2, 31.7, 31.7, 29.8, 29.7, 24.5, 24.4, 22.7, 22.7, 14.2, 14.1. HRMS calcd for $C_{108}H_{118}F_4N_4O_2S_4$: 1707.8107; found: 1707.8100. Anal. calcd for $C_{108}H_{118}F_4N_4O_2S_4$: C, 75.93; H, 6.96; N, 3.28. Found: C, 76.11; H, 6.89; N, 3.34.

Characterization

The ^{1}H NMR and ^{13}C NMR spectra were measured by Bruker AVANCE 300, 400 or 500 MHz spectrometer. Mass spectra was performed by Bruker Daltonics Biflex III MALDI-TOF Analyzer in the MALDI mode. Elemental analyses were measured through a Flash EA 1112 elemental analyzer. Thermogravimetric analysis (TGA) measurements were carried out using a Shimadzu thermogravimetric analyzer (Model DTG-60) under flowing nitrogen gas at a heating rate of 10 °C min^{-1}. The UV-vis absorption spectra were measured using the JASCO-570 spectrophotometer (JASCO. Inc., Japan) in solution (chloroform) and thin film (on a quartz substrate). Electrochemical measurements were carried out under nitrogen in a solution of tetra-*n*-butylammonium hexafluorophosphate ($[^nBu_4N]^+[PF_6]^-$) (0.1 M) in CH_3CN employing a computer-controlled CHI660C electrochemical workstation, a glassy

carbon working electrode coated with SIDIC, DIDIC or TIDIC film, a Ag/AgCl reference electrode, and a platinum-wire auxiliary electrode. The potentials were referenced to a ferrocenium/ferrocene ($FeCp_2^{+/0}$) couple using ferrocene as an external standard. Atomic force microscope (AFM) images were measured on Multimode 8 scanning probe microscopy (Bruker Daltonics, United States) in the tapping mode.

Molecular modelling

Density functional theory (DFT) calculations were performed with the Gaussian 09 program,[S3] using the B3LYP functional. [S4, S5] All-electron double-ξ valence basis sets with polarization functions 6-31G* were used for all atoms.[S6] Geometry optimizations were performed with full relaxation of all atoms in gas phase without solvent effects. The vibrational frequency calculations were performed to check that the stable structures had no imaginary frequency. The molecular geometries used for potential energy surface scan were generated using Molclus.[S7]

GIWAXS and GISAXS measurements

The samples for GIWAXS and GISAXS were prepared on silicon substrates using the same recipe for the devices. The silicon substrates were cleaned successively with deionized water, acetone and isopropanol in an ultrasonic cleaner for 20 min and then treated with oxygen plasma before use. GIWAXS measurements were accomplished with a Xeuss 2.0 SAXS/WAXS laboratory beamline using a Cu X-ray source (8.05 keV, 1.54 Å) and a Pilatus3R 300K detector. The incidence angle is 0.2°. GISAXS measurement was conducted at 19U2 SAXS beamline at Shanghai

Synchrotron Radiation Facility, Shanghai, China, also using the 0.15° incident angle with 10 keV primary beam.

Device fabrication and characterization

All the devices have an inverted sandwich structure, the patterned indium-tin oxide (ITO) glass / ZnO (*ca.* 30 nm)/FTAZ:acceptor/MoO_3 (*ca.* 5 nm)/Ag (*ca.* 80 nm). First, ITO glass (sheet resistance = 15 Ω) was successively pre-cleaned in the ultrasonic bath with de-ionized water, acetone and isopropanol. Then, a ZnO layer was spin-coated at 4000 rpm onto the ITO glass from ZnO precursor solution (prepared by dissolving 0.1 g of zinc acetate dihydrate ($Zn(CH_3COO)_2 \cdot 2H_2O$) and 0.03 mL of ethanolamine ($NH_2CH_2CH_2OH$) in 1 mL of 2-methoxyethanol ($CH_3OCH_2CH_2OH$)), followed by baking at 200 °C for 30 min. The active layer blend (12.0 mg mL^{-1} in chloroform) was spin-coated at 2500 rpm onto the ZnO layer to form the photoactive layer. A MoO_3 layer and Ag layer were then evaporated under vacuum (*ca.* 10^{-5} Pa) to form the anode electrode. The *J-V* curves were measured using a computer-controlled B2912A Precision Source/Measure Unit (Agilent Technologies, United States). An XES-70S1 (SAN-EI Electric Co., Ltd., Japan) solar simulator (AAA grade, 70 mm × 70 mm) coupled with AM 1.5G solar spectrum filters was used as the light source, and the optical power at the sample was 100 mW cm^{-2}. The measured area of the active device was 4 mm^2. A 2 cm × 2 cm monocrystalline silicon reference cell (SRC-1000-TC-QZ) was purchased from VLSI Standards Inc. The EQE spectra were measured using a Solar Cell Spectral Response

Measurement System QE-R3011 (Enlitech Co., Ltd.). The light intensity at each wavelength was calibrated through standard single crystal Si photovoltaic cell.

SCLC measurements

Hole-only or electron-only devices with structures ITO/PEDOT:PSS/active layer/Au for holes and ITO/ZnO/active layer/Ca/Al for electrons were fabricated. The mobility was extracted by fitting the *J-V* curves using SCLC method, $J = (9/8)\mu\varepsilon_r\varepsilon_0 V^2 \exp(0.89(V/E_0 d)^{0.5})/d^3$.[S8]

Here, J refers to the current density, μ is hole or electron mobility, ε_r is relative dielectric constant of the transport medium, which is equal to 3, ε_0 is the permittivity of free space (8.85×10^{-12} F m^{-1}), $V = V_{appl} - V_{bi}$, where V_{appl} is the applied voltage to the device, and V_{bi} is the built-in voltage due to the difference in work function of the two electrodes (for hole-only diodes, V_{bi} is 0.2 V; for electron-only diodes, V_{bi} is 0 V). E_0 is characteristic field, d is the thickness of the active layer and was measured by Dektak XT (Bruker).

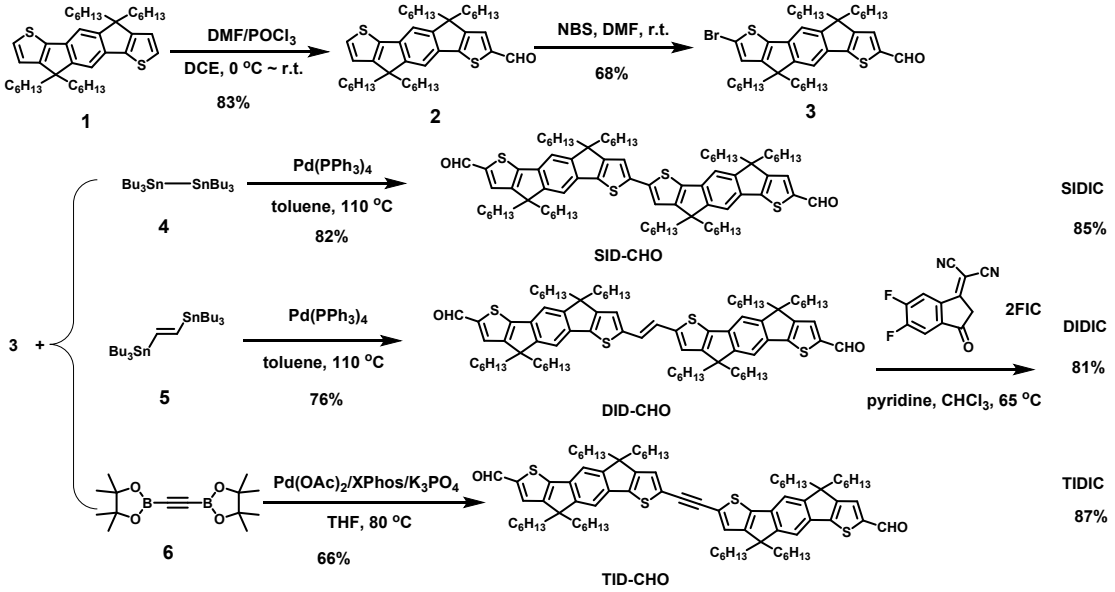

Scheme S1. Synthetic routes to SIDIC, DIDIC and TIDIC.

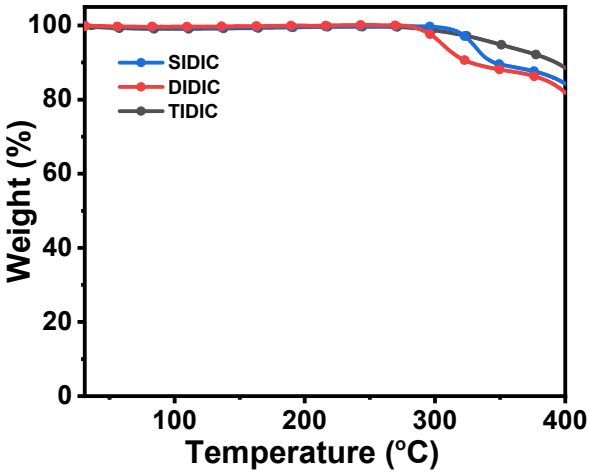

Fig. S1 TGA curves of SIDIC, DIDIC and TIDIC.

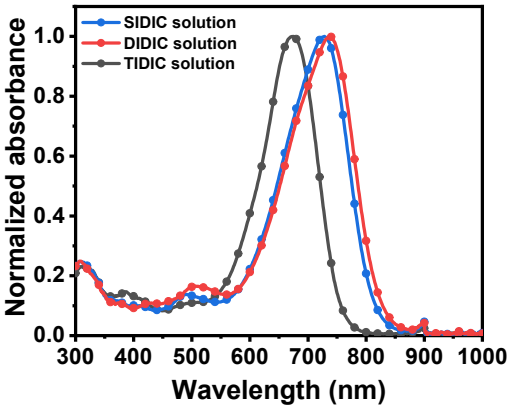

Fig. S2 Absorption spectra of SIDIC, DIDIC and TIDIC in chloroform solution.

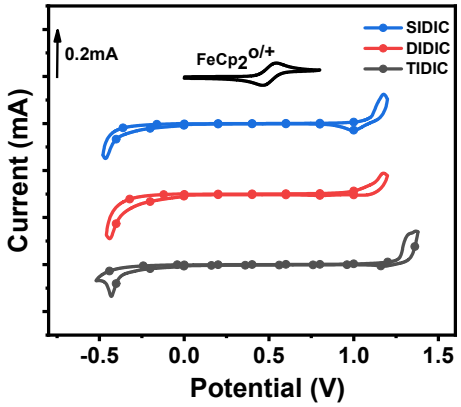

Fig. S3 Cyclic voltammograms for SIDIC, DIDIC and TIDIC in CH_3CN/0.1 M Bu_4NPF_6 at 100 mV s^{-1}; the horizontal scale refers to an Ag/AgCl electrode as a reference electrode.

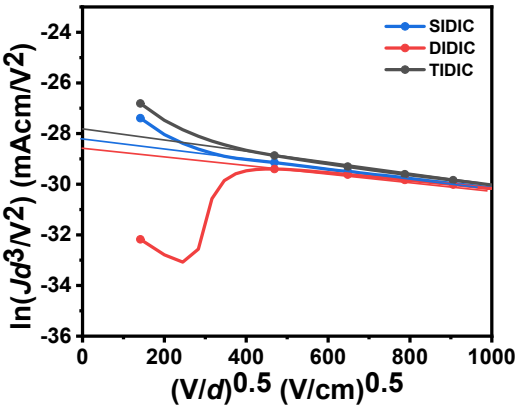

Fig. S4 *J-V* characteristics in the dark for electron-only devices based on SIDIC, DIDIC and TIDIC.

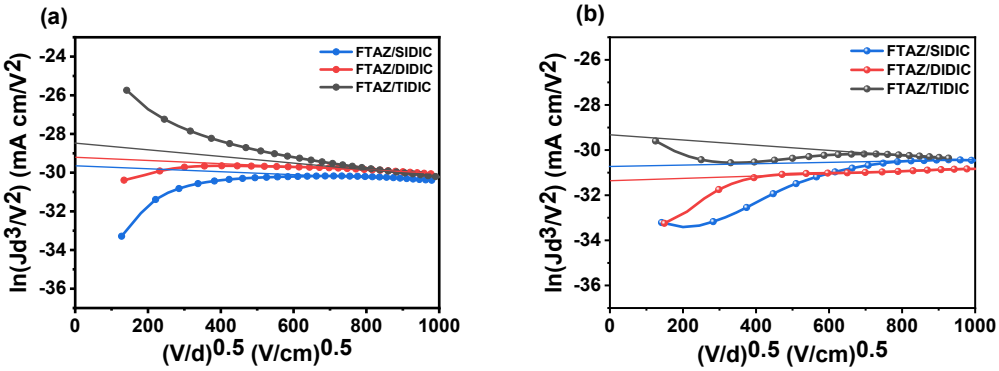

Fig. S5 *J-V* characteristics in the dark for (a) hole-only and (b) electron-only devices based on FTAZ/acceptor blends.

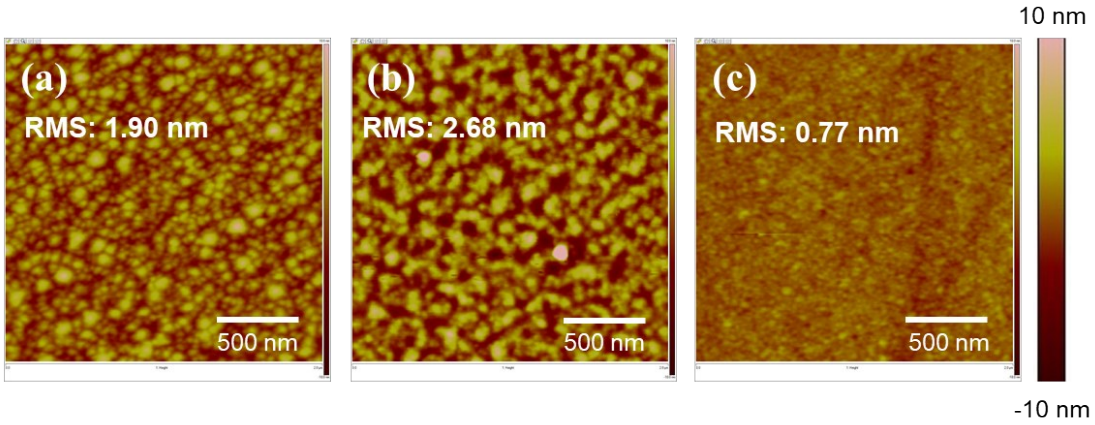

Fig. S6 AFM height images of (a) SIDIC, (b) DIDIC and (c) TIDIC pure films.

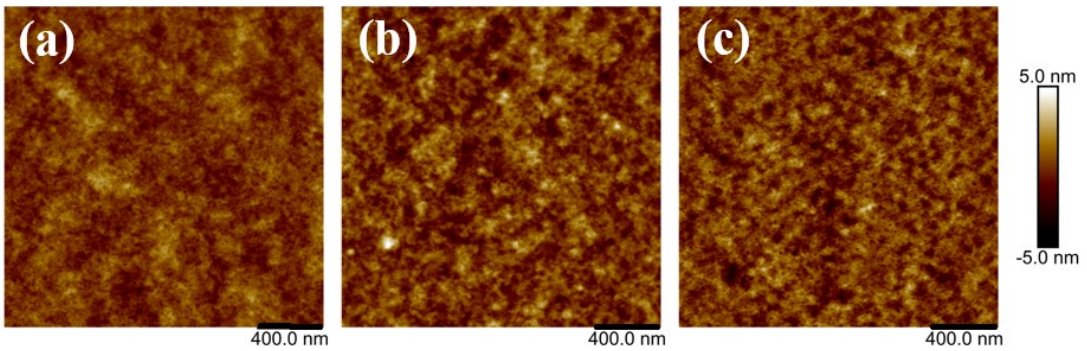

Fig. S7 AFM height images of (a) FTAZ/SIDIC, (b) FTAZ/DIDIC and (c) FTAZ/TIDIC blends under optimized device conditions.

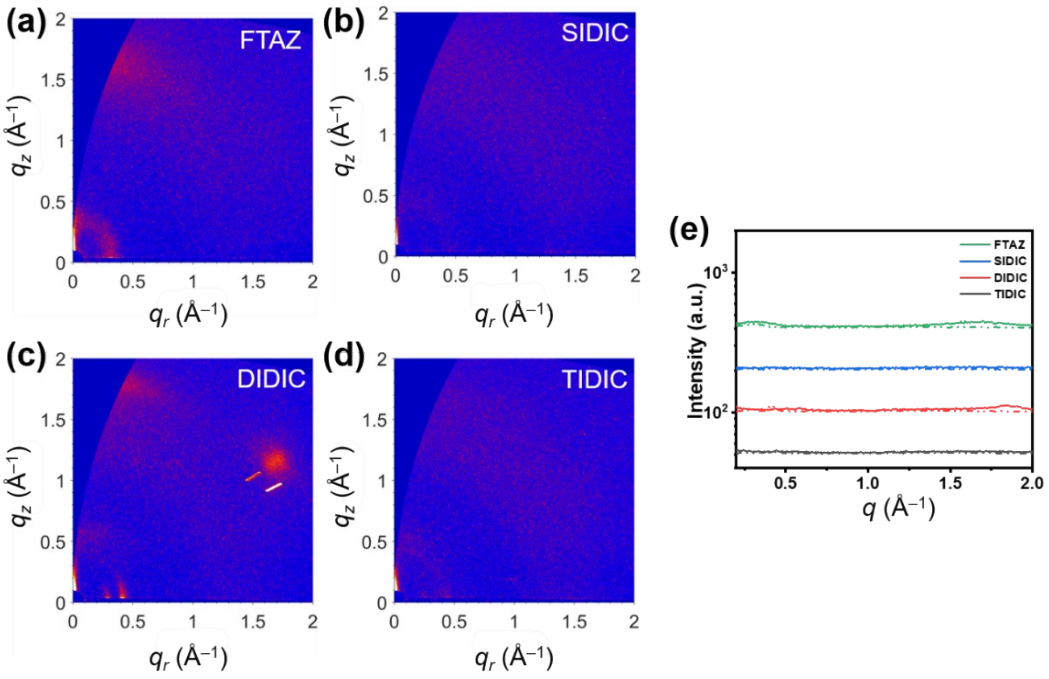

Fig. S8 2D GIWAXS patterns of (a) FTAZ, (b) SIDIC, (c) DIDIC and (d) TIDIC pure films; (e) the corresponding intensity profiles along the in-plane (dashed line) and out-of-plane (solid line) directions.

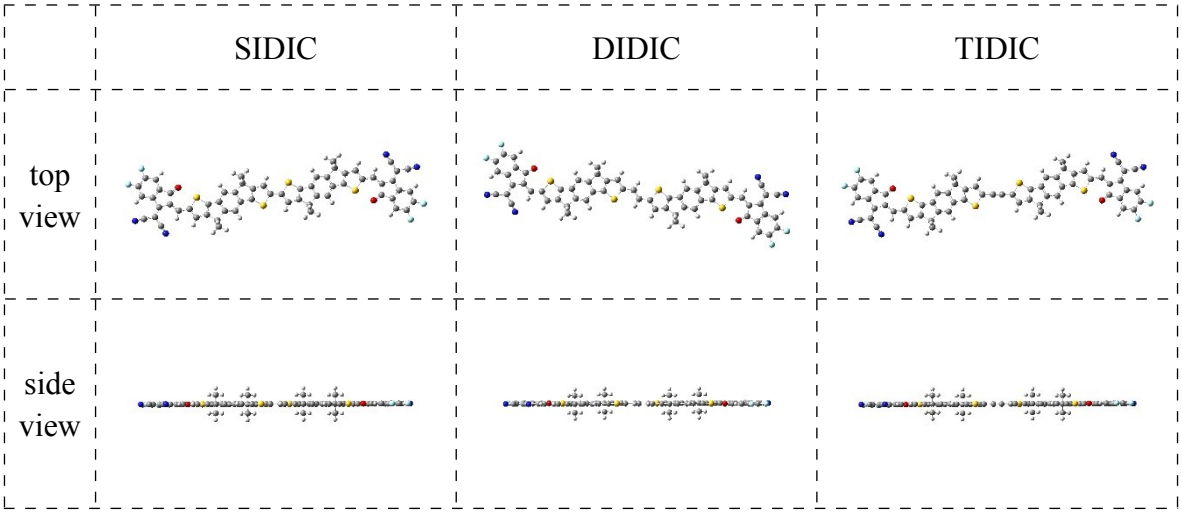

Fig. S9 The optimal geometries of SIDIC, DIDIC and TIDIC (alkyls are simplified to methyl) calculated at B3LYP/6-31G* level.

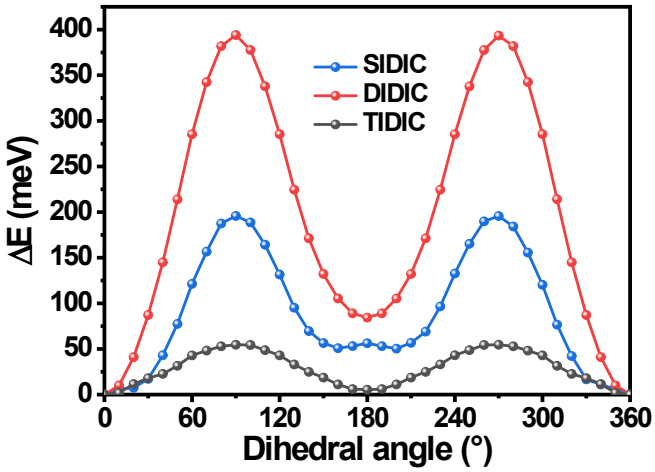

Fig. S10 Potential energy surface scan with the dihedral angles between two IDT planes in SIDIC, DIDIC and TIDIC.

Table S1 Device data of as-cast OSCs based on FTAZ/acceptor with different D/A ratio

acceptor	D/A (w/w)	V_{OC}[a] (V)	J_{SC}[a] (mA cm^{-2})	FF[a] (%)	PCE[a] (%)
SIDIC	1/1	0.879 (0.881±0.004)	16.2 (14.7±1.0)	61.6 (58.4±1.8)	8.8 (7.6±0.7)
	1/1.5	0.857 (0.881±0.005)	17.3 (17.5±0.3)	68.3 (65.8±1.4)	10.1 (9.9±0.1)
	1/1.8	0.818 (0.821±0.004)	17.4 (17.9±0.6)	48.2 (45.9±2.3)	6.9 (6.8±0.1)
DIDIC	1/1	0.834 (0.805±0.009)	14.4 (15.1±0.7)	58.4 (55.0±3.4)	7.0 (6.6±0.4)
	1/1.5	0.816 (0.810±0.005)	16.8 (16.7±0.1)	62.1 (60.4±2.3)	8.5 (8.2±0.3)
	1/1.8	0.803 (0.802±0.003)	16.7 (17.3±0.7)	61.4 (58.5±1.9)	8.2 (8.1±0.2)
TIDIC	1/1	0.899 (0.891±0.005)	17.0 (17.1±0.1)	64.2 (63.5±0.5)	9.8 (9.7±0.1)
	1/1.5	0.883 (0.876±0.007)	18.0 (18.1±0.3)	70.0 (66.8±4.1)	11.1 (10.6±0.7)
	1/1.8	0.881 (0.868±0.009)	18.4 (17.9±0.5)	60.5 (60.7±1.0)	9.8 (9.5±0.3)

[a] Average values (in parenthesis) are obtained from 20 devices.

Table S2 Device data of the OSCs based on FTAZ/acceptor (D/A=1/1.5) with different DIO content in chloroform

acceptor	DIO (%)	V_{OC}[a] (V)	J_{SC}[a] (mA cm^{-2})	FF[a] (%)	PCE[a] (%)
SIDIC	0.2	0.863 (0.858±0.005)	18.4 (17.9±0.3)	69.4 (68.4±1.4)	11.0 (10.5±0.3)
DIDIC	0.2	0.816 (0.817±0.001)	17.5 (17.1±0.3)	65.1 (64.0±1.0)	9.3 (8.9±0.3)
TIDIC	0.1	0.874 (0.878±0.007)	19.6 (19.0±0.6)	71.4 (69.0±1.8)	12.3 (11.5±0.5)
	0.2	0.879 (0.869±0.006)	20.2 (20.6±0.4)	73.6 (70.7±1.4)	13.1 (12.7±0.2)
	0.3	0.874 (0.867±0.005)	19.0 (19.0±0.4)	72.8 (70.7±1.4)	12.1 (11.6±0.3)

[a] Average values (in parenthesis) are obtained from 20 devices.

Table S3 Charge mobilities of pure and blend films measured by SCLC method

active layer	μ_h (10^{-3} cm^2 V^{-1} s^{-1})	μ_e (10^{-3} cm^2 V^{-1} s^{-1})	μ_h/μ_e
SIDIC	–	3.4	–
DIDIC	–	2.2	–
TIDIC	–	4.9	–
FTAZ/SIDIC	0.75	0.29	2.6
FTAZ/DIDIC	1.2	0.14	8.6
FTAZ/TIDIC	2.5	1.1	2.3

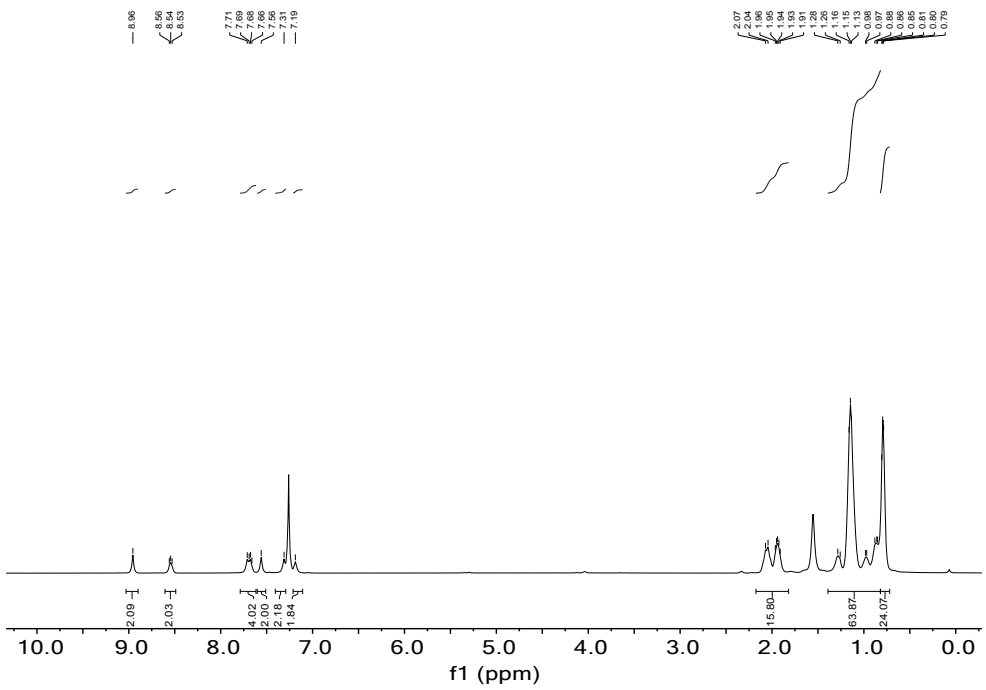

^{1}H NMR for SIDIC

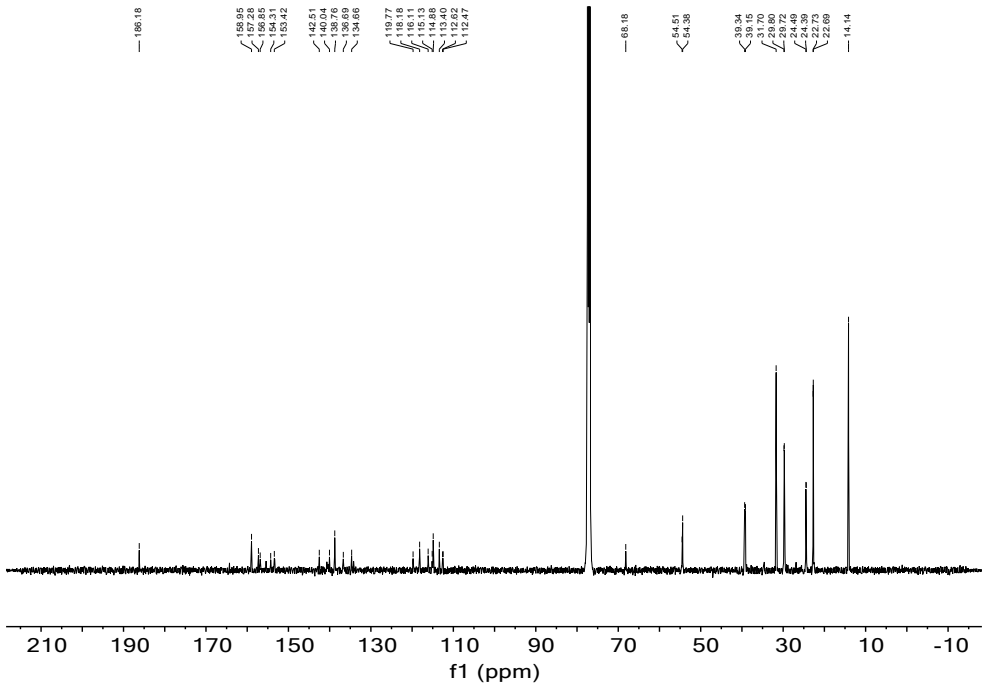

^{13}C NMR for SIDIC

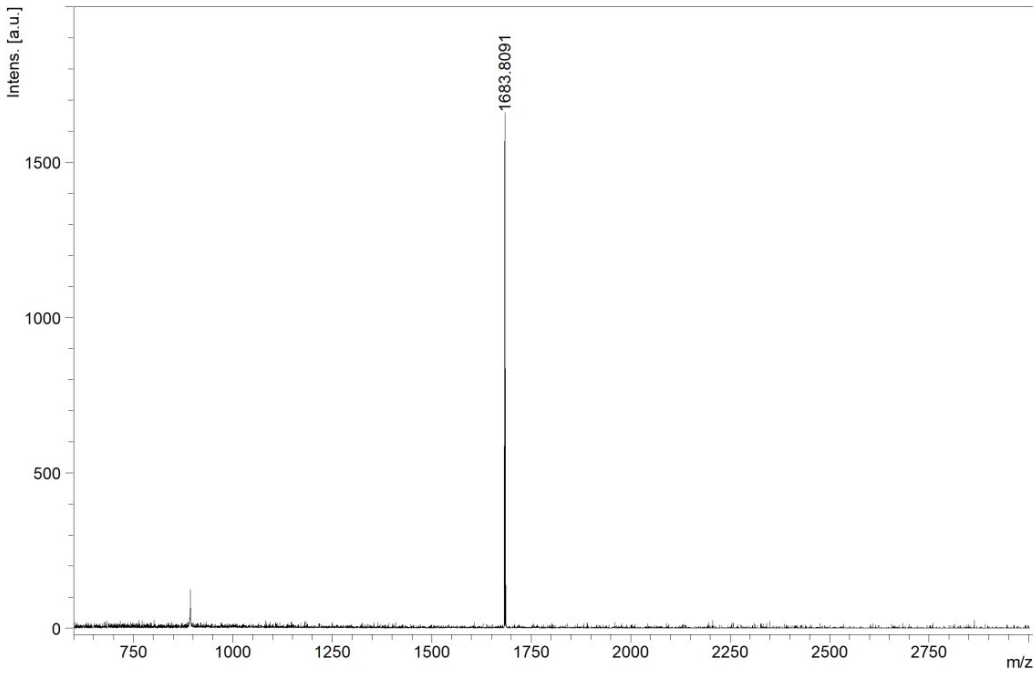

HRMS for SIDIC

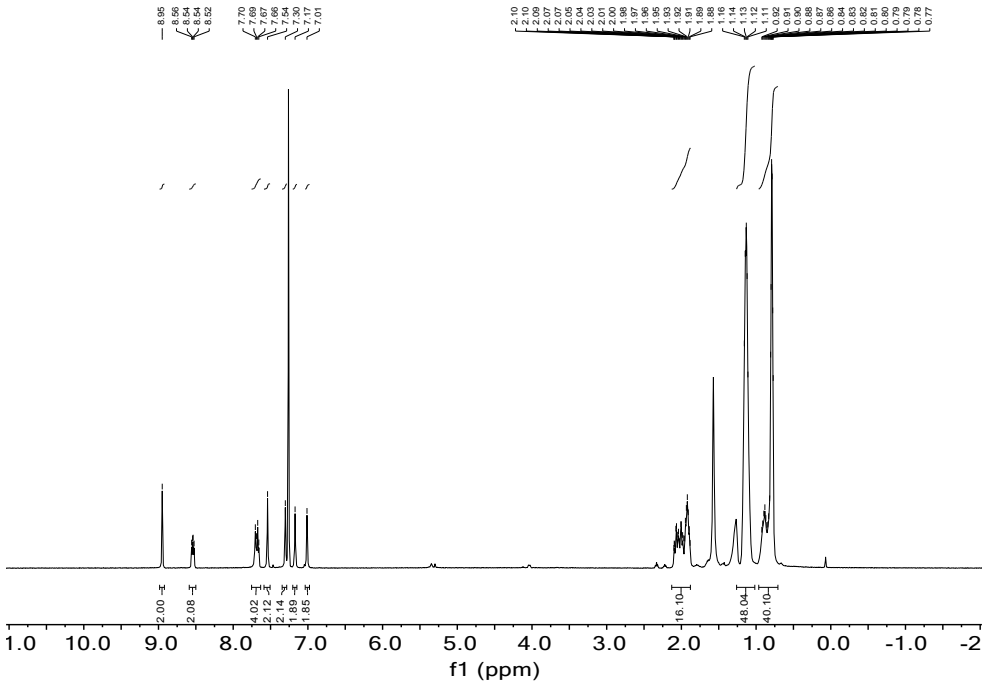

^{1}H NMR for DIDIC

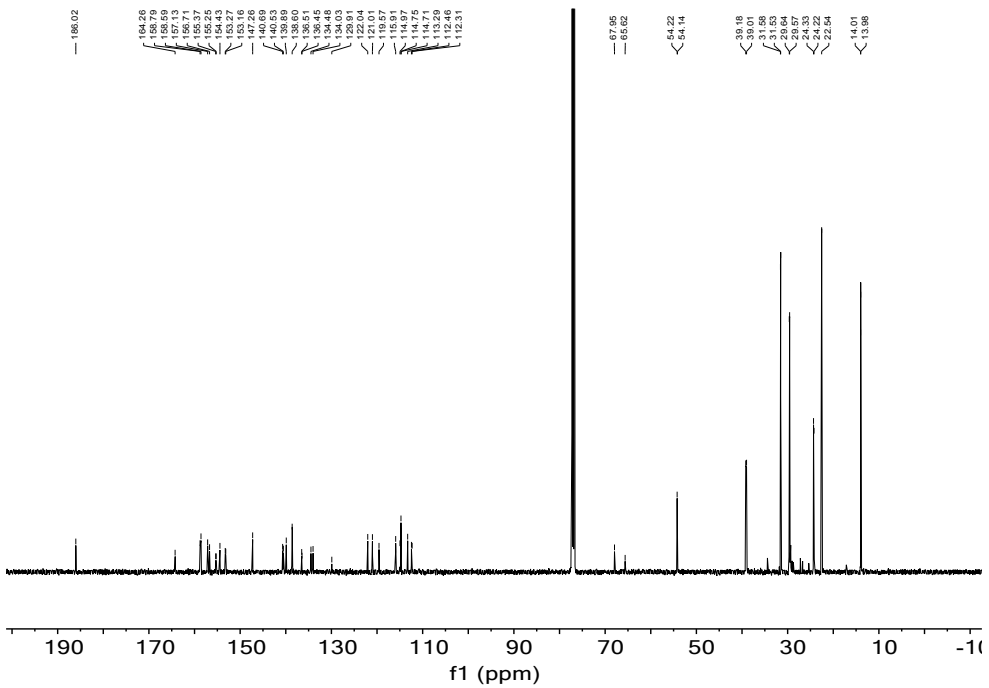

^{13}C NMR for DIDIC

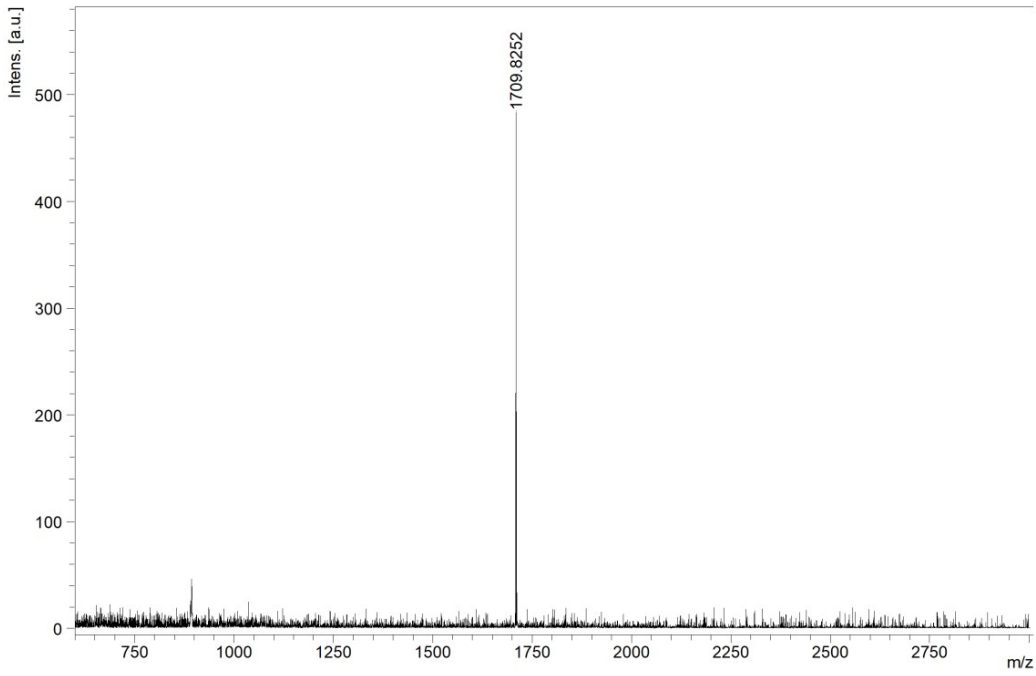

HRMS for DIDIC

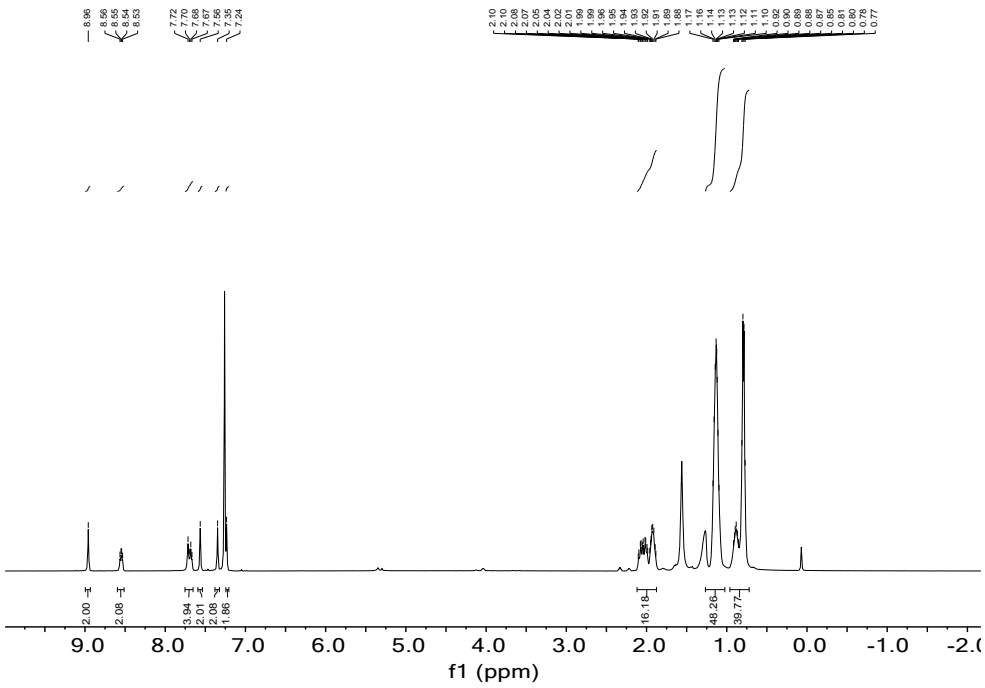

^{1}H NMR for TIDIC

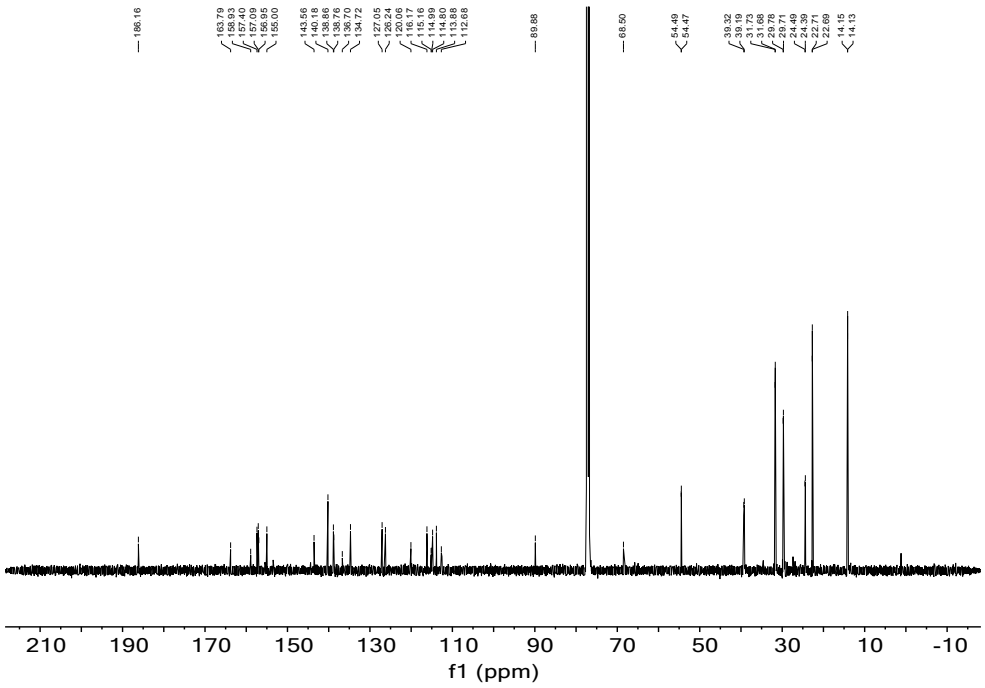

^{13}C NMR for TIDIC

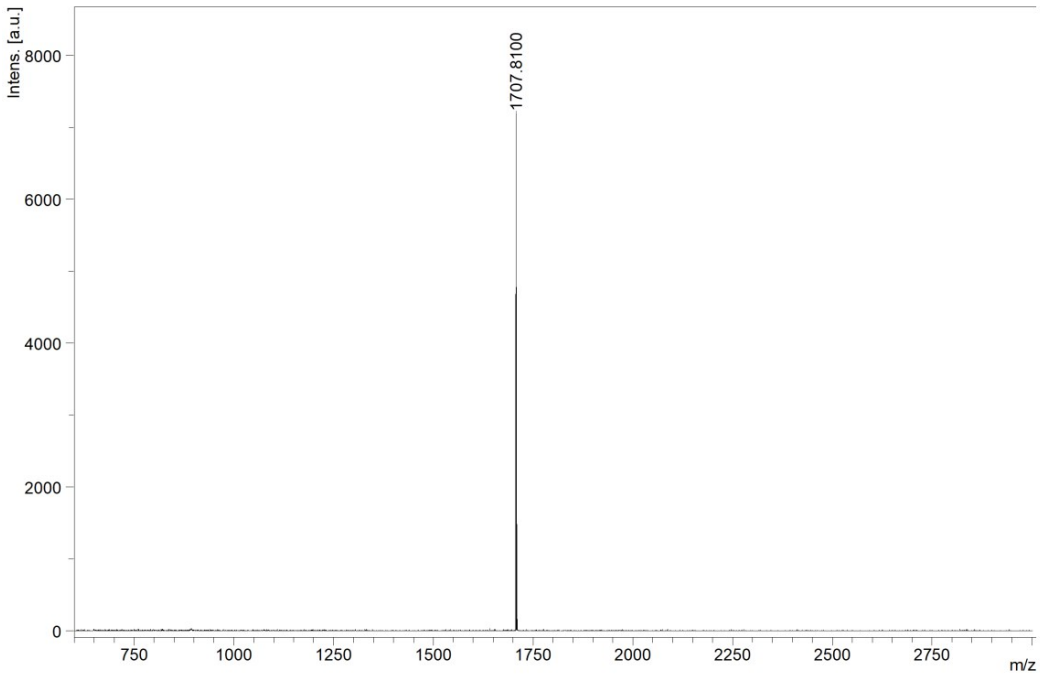

HRMS for TIDIC

References:

S1 S. Dai, F. Zhao, Q. Zhang, T. K. Lau, T. Li, K. Liu, Q. Ling, C. Wang, X. Lu, W. You, X. Zhan, *J. Am. Chem. Soc.*, 2017, **139**, 1336-1343.

S2 S. C. Price, A. C. Stuart, L. Yang, H. Zhou, W. You, *J. Am. Chem. Soc.*, 2011, **133**, 4625-4631.

S3 M. J. Frisch, G. W. Trucks, H. B. Schlegel, G. E. Scuseria, M. A. Robb, J. R. Cheeseman, G. Scalmani, V. Barone, B. Mennucci, G. A. Petersson, H. Nakatsuji, M. Caricato, X. Li, H. P. Hratchian, A. F. Izmaylov, J. Bloino, G. Zheng, J. L. Sonnenberg, M. Hada, M. Ehara, K. Toyota, R. Fukuda, J. Hasegawa, M. Ishida, T. Nakajima, Y. Honda, O. Kitao, H. Nakai, T. Vreven, J. A. Montgomery Jr., J. E. Peralta, F. Ogliaro, M. J. Bearpark, J. Heyd, E. N. Brothers, K. N. Kudin, V. N. Staroverov, R. Kobayashi, J. Normand, K. Raghavachari, A. P. Rendell, J. C.

Burant, S. S. Iyengar, J. Tomasi, M. Cossi, N. Rega, N. J. Millam, M. Klene, J. E. Knox, J. B. Cross, V. Bakken, C. Adamo, J. Jaramillo, R. Gomperts, R. E. Stratmann, O. Yazyev, A. J. Austin, R. Cammi, C. Pomelli, J. W. Ochterski, R. L. Martin, K. Morokuma, V. G. Zakrzewski, G. A. Voth, P. Salvador, J. J. Dannenberg, S. Dapprich, A. D. Daniels, O¨. Farkas, J. B. Foresman, J. V. Ortiz, J. Cioslowski and D. J. Fox, Gaussian, Inc., Wallingford, CT, USA, 2009.

S4 C. Lee, W. Yang and R. G. Parr, *Phys. Rev. B*, 1988, **37**, 785–789.

S5 A. D. Becke, *J. Chem. Phys.*, 1993, **98**, 5648–5652.

S6 R. Krishnan, J. S. Binkley, R. Seeger and J. A. Pople, *J. Chem. Phys.*, 1980, **72**, 650–654.

S7 T. Lu Molclus program, Version 1.9.5, http://www.keinsci.com/research/molclus.html (accessed 2020-Jun-1).

S8 G. G. Malliaras, J. R. Salem, P. J. Brock and C. Scott, *Phys. Rev. B*, 1998, **58**, 13411-13414.